

Is the neutral surface really neutral?

A close examination of energetics of along isopycnal mixing

Rui Xin Huang

Department of Physical Oceanography
Woods Hole Oceanographic Institution
Woods Hole, MA 02543, USA

April 19, 2010

Abstract

The concept of along-isopycnal (along-neutral-surface) mixing has been one of the foundations of the classical large-scale oceanic circulation framework. Neutral surface has been defined a surface that a water parcel move a small distance along such a surface does not require work against buoyancy.

A close examination reveals two important issues. First, due to mass continuity it is meaningless to discuss the consequence of moving a single water parcel. Instead, we have to deal with at least two parcels in discussing the movement of water masses and energy change of the system. Second, movement along the so-called neutral surface or isopycnal surface in most cases is associated with changes in the total gravitational potential energy of the ocean.

In light of this discovery, neutral surface may be treated as a preferred surface for the lateral mixing in the ocean. However, there is no neutral surface even at the infinitesimal sense. Thus, although approximate neutral surfaces can be defined for the global oceans and used in analysis of global thermohaline circulation, they are not the surface along which water parcels actually travel. In this sense, thus, any approximate neutral surface can be used, and their function is virtually the same. Since the structure of the global thermohaline circulation change with time, the most suitable option of quasi-neutral surface is the one which is most flexible and easy to be implemented in numerical models.

1. Introduction

The ocean is a turbulent environment; thus, simulating the oceanic circulation is directly linked to the simulation of turbulence over broad spatial and temporal scales. Due to the limitation of computer power all numerical models are based on different kinds of subscale parameterizations, including the parameterization of the horizontal and vertical diffusion of tracers and dissipation for the momentum. All parameterizations are the results of combining our knowledge gained from observations and theoretical reasoning.

Due to the technical difficulties of observing momentum dissipation, the corresponding parameterization of momentum in numerical models has been progressing in a very low pace. Recent study has been mostly focused on the diapycnal diffusivity of the tracers, such as temperature and salinity. On the other hand, the horizontal (or isopycnal) diffusion of tracers has not received the due attention. Although we may admit that isopycnal mixing may not be isotropic or homogeneous, the common practice in most numerical models is still treated it as isotropic and homogeneous.

The concept of potential density surface or neutral surface has been widely used in physical oceanography. The common wisdom is that fluid parcels can move along neutral density surface without doing work against gravitational force. In addition, in most existing numerical models, the along isopycnal mixing is assumed to be isentropic.

In this study, we will show that water parcels traveling along a potential density or a neutral surface may involve with change of gravitational potential energy. As a consequence, along isopycnal mixing is not isentropic.

The neutral surface has been defined as following: “Neutral surfaces are defined so that small isentropic and adiabatic displacements of a fluid parcel in a neutral surface do not produce a buoyancy restoring force on the parcel.” (McDougall, 1987); “A neutral trajectory is a three-dimensional path in the ocean, and is defined such that no buoyancy forces act on a water parcel when it is moved a small distance along this path.” (Eden and Willebrand, 1999).

A critically important point is that one cannot talk about the consequence of moving a single parcel alone in the ocean. Assume that a water parcel A, originally located on $p=500$ db level, moves away from its original location along certain density (either a potential density or a neutral density) surface and reaches a new location, say at the $p=1000$ db level, Fig. 1a. As a result, parcel B originally sits in this location is now repelled from its original location. In addition, there is an empty space left behind in the 500 db level, as shown in Fig. 1b. Due to continuity other water parcels must come to fill up this space. A simple choice is to let parcel B fills up this empty place, and this involves the position switch between two parcels. Other choices must involve multi-parcel position exchanges.

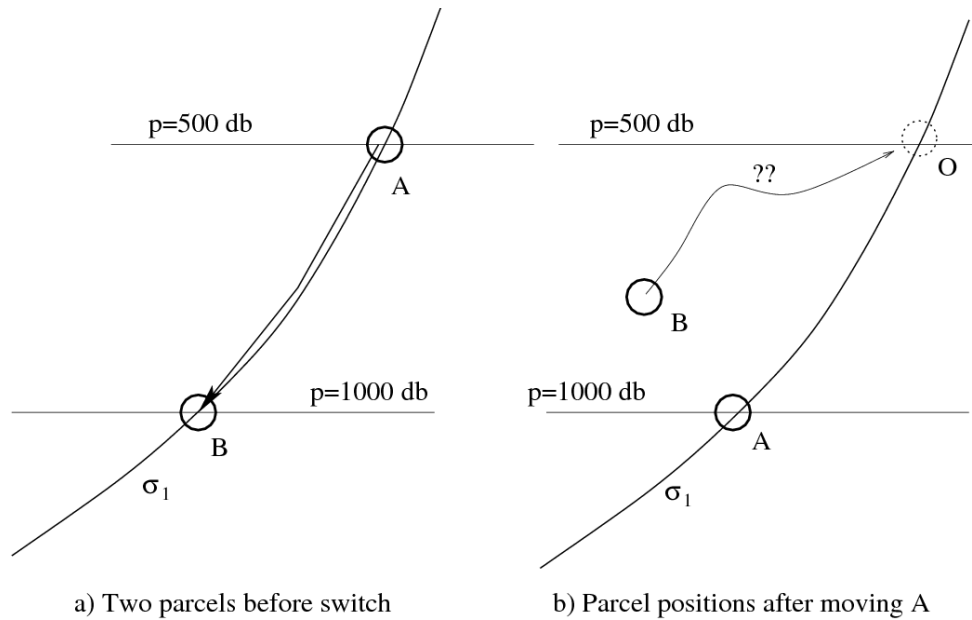


Fig. 1. Movement of a water parcel and its consequence.

Thus, it is meaningless talking about GPE change of a single water parcel only. Instead, we must examine the total GPE change in the system associated with movements of the relevant water parcels. Due to continuity of water mass, for any movement of a water parcel, there are at least two water parcels involving in the change of location, and thus the corresponding change of GPE. In the following analysis we will discuss the simplest case, i.e., the change of GPE associated with exchange of two water parcels.

2. Two examples demonstrating the basic physics

First, we examine the exchange of two parcels along the intersection (indicated by the horizontal red line with arrow, labeled as \vec{s} in Fig. 2) between the pressure surface P (with constant pressure p , green lines) and a potential surface σ_p (black), which is defined using reference pressure p . Although these two parcels have different temperature and salinity, they have the same in-situ density under pressure p . Since they also sit on the same pressure surface, exchange of these two parcels does not change their in-situ density at their new locations. Thus, exchange along line \vec{s} does not change the GPE of the system.

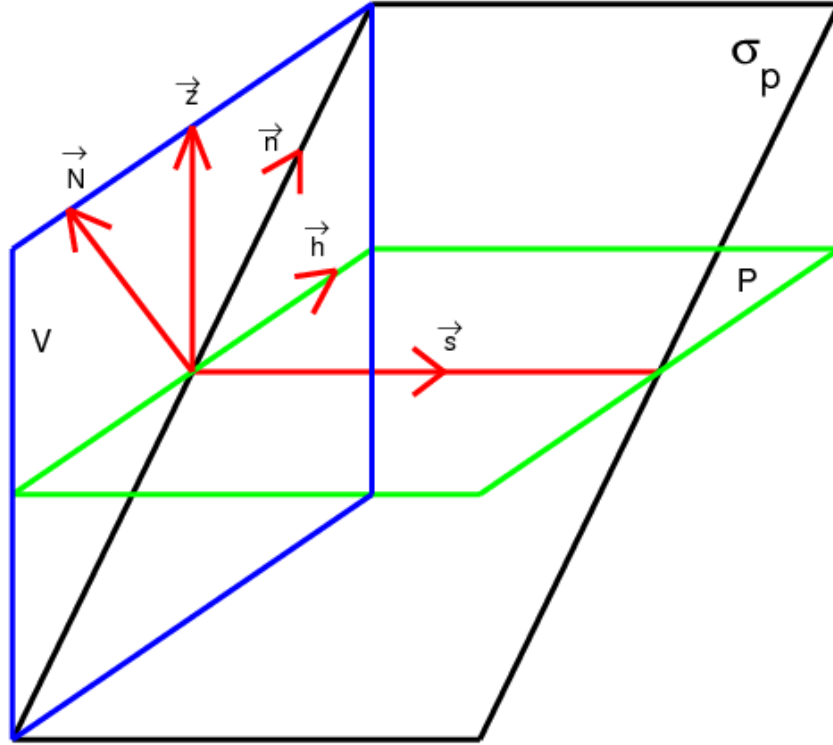


Fig. 2. Sketch of the pressure surface (green) and potential density surface (black).

There is however a possibility that the stratification at the corresponding original locations associated with these two parcels may be changed because these two parcels have different temperature and salinity, and thus have different potential temperature. (Following the common practice, potential temperature is defined, using the sea surface as the reference level.) In addition, due to cabbeling effect when the mixture of these two parcels mix will have a density heavier than the original parcels. Therefore, the total volume of the water parcels shrink, the corresponding centers of water columns above these parcels move downward. As a result, the total GPE of the system is reduced. However, we will not discuss the change of GPE associated with cabbeling in this study, and main point relevant to our study here is that water parcels along this line can be exchanged without doing work in the gravitational field, i.e., water parcels can travel freely along this line.

Our next step is to examine what happens if parcels are exchanged in all potential direction in a plane V perpendicular to the vector \vec{s} , marked by the blue lines Fig. 2. On this plane, we can identify at least four vectors: the “horizontal vector \vec{h} ”, the normal vector \vec{N} of the potential density surface σ_p , a vector \vec{n} which is on the potential density surface and perpendicular to both vectors \vec{s} and \vec{N} . In addition, there is a vector \vec{z} which is opposite to the direction of gravitational force.

It is well known that mixing along the direction of \vec{N} or \vec{z} requires doing work against gravitational force; thus, our focus here is to examine what happens in the vicinity of vector \vec{n} . We will take a plane view looking from the left side to right side (or vice versa) of Fig. 2. The following two figures, Figs. 3 and 4, are sketches based on diagnosis of what happens in the world oceans, based on WOA01 dataset, with one-by-one degree resolution.

The first example is a meridional section through a station at (30.5°W, 48.5°S). We also choose $p=1000\text{db}$ as the pivotal pressure level denoted as the horizontal line passing point O in Fig. 3, and the stratification at this station is denoted as the vertical line through point O; the corresponding pivotal potential density surface is σ_{1000} . This station is within the strong front of Antarctic Circumpolar Current (ACC), so that this potential density surface slopes up southward. At station S, one degree south of station O, the σ_{1000} surface is located at a depth of 873.0db; the constant in-situ density surface passing through point O interests the water column at station S at depth of 989.4db. We can also find another potential density surface $\sigma_{873.4}$, which is based on reference pressure 873.4 db and passing through point P at depth of 873.4db at station S and point O.

Let us examine density perturbations induced by exchanging two water parcels: parcel O originally locates at point O, and parcel UL originally locates at the upper, upper left, or left side of parcel O. Density and its perturbations associated with parcel exchanges as a function of the angle are schematically shown in the right panel of Fig. 3.

Starting from the vertical position, thin red and blue curves depict density (denoted as the radius from origin O) of parcel O and UL as a function of the angle θ . Since for large-scale circulation the stratification is stable, for a water parcel pair with parcel UL above parcel O (near line OU), parcel O is heavier than parcel UL. If we exchange their position, density of parcel O, denoted as $\rho(O \rightarrow UL)$, declines during its upward motion; thus, the heavy red line is below the thin blue line, i.e., $\rho(O \rightarrow UL) < \rho(O)$. However, when parcel O arrives at the original location of parcel UL, the corresponding density anomaly is positive, i.e., $\rho(O \rightarrow UL) > \rho(UL)$. The corresponding new density of parcel UL during this exchange is denoted as $\rho(UL \rightarrow O)$. Due to compression associated with the downward motion, its density increases, and it satisfies $\rho(UL) < \rho(UL \rightarrow O) < \rho(O \rightarrow UL)$, shown in the right part of Fig. 3b.

A most important physical point is as follows. When the newly arriving parcel has a density lighter (heavier) than the corresponding density of the original parcel at the same location, water column above is pushed upward and gravitational potential energy is increased (reduced). Thus external source of mechanical energy is required for the case when density perturbation is negative; on the other hand, if density perturbation is positive, gravitational potential energy is released. It is to emphasize that gravitational potential release during the process of water parcel exchange is mostly dissipated through turbulence and internal waves. Although a very small portion of such energy released may contribute to the increase of gravitational potential energy of the whole system, it is practically all lost through turbulent dissipation, and we will omit such contribution in the following discussion.

As we turn the angle anticlockwise, the density perturbations decline in their amplitude, Fig. 3b. Potential density surface σ_{1000} (denoted as the thick black line) is the critical boundary of the domain discussed above, and it interests the water column at station S at point A with $p=873.0$ db, Fig. 3a. By definition, all parcels on the σ_{1000} surface should have the same in-situ density when they arrive at pressure level 1000db; thus, a parcel moving from the upper left part to the origin O of this diagram should have the same in-situ density as the water parcel originally locates in point O, i.e., $\rho(UL \rightarrow O) = \rho(O)$ and the blue lines intersect, Fig. 3b.

However, after the exchange parcel O have an in-situ density larger than the original in-situ density at the upper left part of this diagram, i.e., $\rho(O \rightarrow UL) > \rho(UL)$, and this fact is indicated by the distance between intersection of the heavy black line with thin red curve and heavy curve. Thus, if these two water parcels in a slanted water column (represented by the thick black line in this diagram) exchange their position, the volume will shrink and the total gravitational potential energy of the pair will be reduced, i.e., energy will be released.

As we turn the angle further anticlockwise, $\rho(UL \rightarrow O) - \rho(O)$ becomes positive, but $\rho(O \rightarrow UL) - \rho(UL)$ continues to decline. Potential density surface $\sigma_{873.4}$ is the second critical boundary, which is defined by satisfying the constraint $\rho(O \rightarrow UL) = \rho(UL)$; thus, by definition, p=873.4 db (point P in Fig. 3a) is the level where the neutral surface should intersect the water column at this station. This is due to the definition of neutral surface that when arriving at this station the water parcel starting from station O should have the same in-situ density as the water parcel originally sit there. However, at this boundary we have $\rho(UL \rightarrow O) > \rho(O)$, Table 1. That is to say the water parcel originated from station S should have an in-situ density heavier than the original in-situ density at station O. Therefore, gravitational potential energy will be released, if two water parcels belong to these two stations are exchanged. Since we are talking about the reversible adiabatic position exchange only, the pathways do not matter. Thus, within the angle between σ_{1000} and $\sigma_{873.4}$ water parcel pair exchange leads to the release of gravitational potential energy, so thus mixing can take place freely.

If we continue to rotate the angle anticlockwise, $\rho(O \rightarrow UL) < \rho(UL)$. This implies that external source of mechanical energy is required for supporting the increase of gravitational potential energy associated with the upward pushing of water column. Note that we omit the contribution due to water column shrink associated with moving the water parcel from upper left to point O.

At the very end of this angle rotation, a boundary associated with the in-situ density surface is reached (thin solid lines in Fig. 3a and 3b.) Although $\rho(O \rightarrow UL) < \rho(UL)$ suggests that there is gravitational potential energy released, it is mostly dissipated through turbulence, as discussed above. A further increase in $\rho(UL \rightarrow O) - \rho(O)$ indicates that more energy is required for sustaining the mixings; thus, it is clear that water parcel exchange along this line requires external source of mechanical energy for supporting.

Our analysis above is based on a finite distance between two stations. If the distance between these stations is gradually reduced to infinitesimal, these two potential density surface will collapse into one, i.e., potential surface σ_{1000} . From our analysis above we conclude that at this station and near pressure level 1000 db, parcels can be exchanged along directions \vec{s} and \vec{n} freely without requiring external source of mechanical energy for supporting.

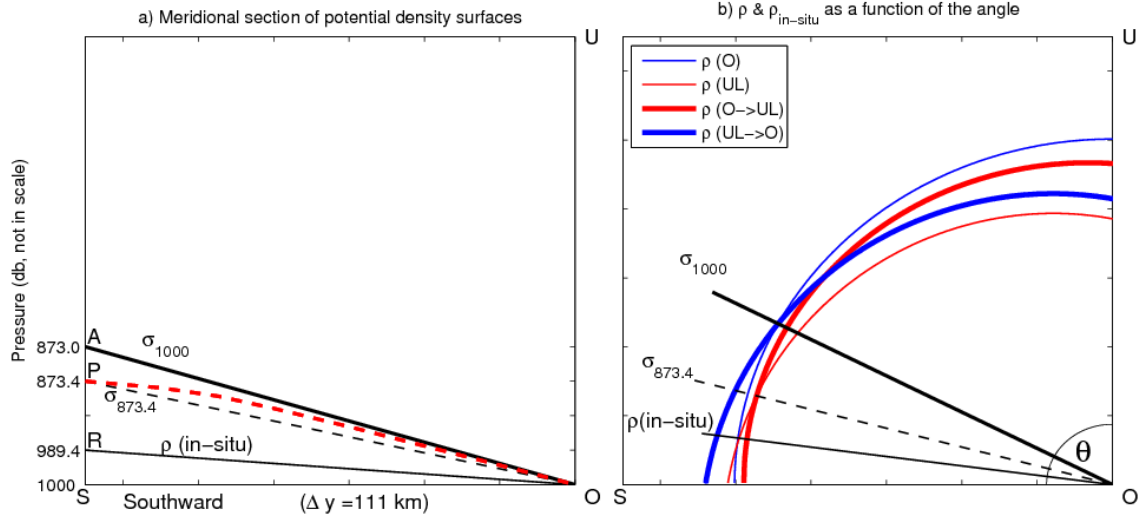


Fig. 3. Sketch of potential density surface (left panel); density at the new location after exchange, as compared with the local in-situ density (right panel). Calculations are based on a meridional section along 30.5°W at 49.5°S and 48.5°S taken from WOA01 data.

Point	p (db)	σ_p	$\sigma_{1000}(O) - \sigma_t(p)$	$\sigma_{1000}(p) - \sigma_{1000}(O)$	$\sigma_{1000}(p) - \sigma_t(p)$
A	873.0288	31.70323	0.584658	0.000000	0.000174
P	873.4128	31.70500	0.582714	0.000174	0.000000
R	989.4128	32.23904	0.000000	0.048718	-0.048672

Table 1. Density and its perturbations at three critical boundaries for the meridional section presented in Fig. 3, density in unit of kg/m^3 .

As a second example, we discuss the situation at a station (149.5°E , 20.5°N), and the σ_{1000} potential surface is chosen as the pivotal potential density surface again. A meridional section is shown in Fig. 4. The situation in this station is similar to that shown in Fig. 3. The major difference is that here the potential density surface σ_{1000} intersects the water column at the station south of station O at a pressure level lower than that of potential density surface based on local pressure, $\sigma_{983.518}$, Fig. 4a.

As discussed above, we gradually rotate the angle of mixing water parcel pair. Starting from the vertical direction, the corresponding density perturbations are similar to the case shown in Fig. 3b. Since potential surface $\sigma_{983.518}$ lies above potential surface σ_{1000} , density perturbations associated with these two boundaries are opposite to that discussed in Fig. 3b.

By definition, when parcel O moved to the upper left part along the $\sigma_{983.518}$ surface, it should have the same density as the local water parcel. However, water parcel moved from the upper left part to point O will have a density smaller than the local density, as shown in Fig. 4b and Table 2. As we continue rotate the angle of mixing pair from potential surface $\sigma_{983.518}$ to potential surface σ_{1000} , $\rho(O \rightarrow UL) - \rho(UL)$ becomes negative, as shown in Fig. 4b and Table 2. On the other hand, by definition of σ_{1000} , parcel moved from the upper left part to point O should have the same density as the local parcel. Thus, within the wedge defined by $\sigma_{983.518}$ and

σ_{1000} water parcel exchange will lead to a negative density anomaly, and thus external mechanical energy is required for sustaining this exchange.

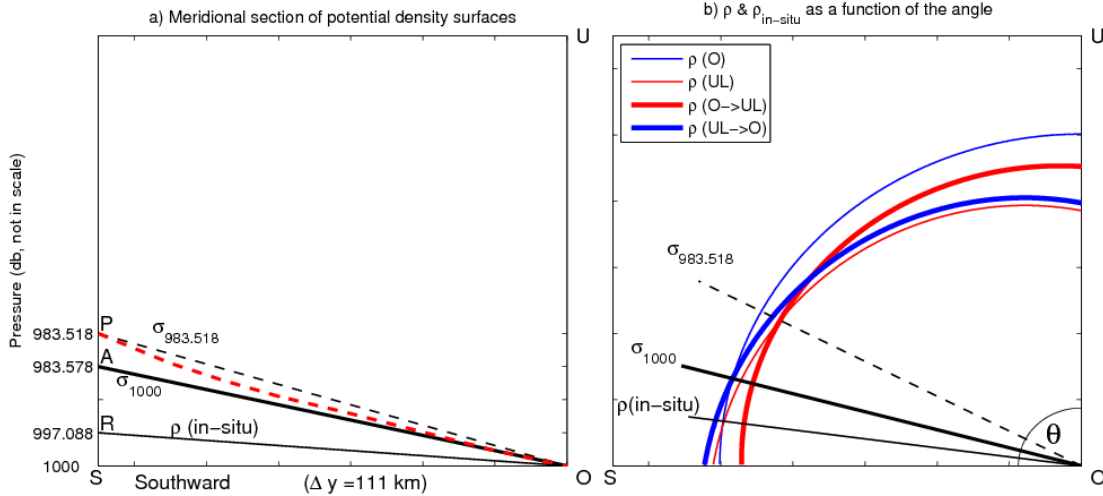


Fig. 4. Sketch of potential density surface (left panel); density at the new location after exchange, as compared with the local in-situ density (right panel). Based on a meridional section along 149.5°E at 19.5°N and 20.5°N taken from WOA01 data.

Point	p (db)	σ_p	$\sigma_{1000}(O) - \sigma_t(p)$	$\sigma_{1000}(p) - \sigma_{1000}(O)$	$\sigma_{1000}(p) - \sigma_t(p)$
P	983.5180	31.87090	0.075045	-0.000058	0.000000
A	983.5776	31.87117	0.075715	0.000000	-0.000058
R	997.0880	31.93269	0.000000	0.013249	-0.012335

Table 2. Density and its perturbations at three critical boundaries for the meridional section presented in Fig. 4, density in unit of kg/m^3 .

The density anomaly diagnosed from the above calculation is consistent with the corresponding changes in compressibility. As shown in Table 3, the density anomaly is equal to the compressibility difference multiplied by the pressure difference.

Longitude	Latitude	p (db)	$\delta\rho$ (kg/m^3)	δp (db)	δK_η ($10^{-6} / \text{db}$)	$\delta\rho = \bar{\rho}\delta p \cdot \delta K_\eta$ (kg/m^3)
30.5W	49.5S	873.4	-0.000174	126	-0.00133	-0.0000175
149.5E	20.5N	983.6	0.0000582	16.4	0.00344	0.0000582

Table 3. Changes in density, pressure level and compressibility for the two stations shown in Figs. 2 and 3.

3. Connection with compressibility

It is well known that sea water is slightly compressible, and its compressibility depends on temperature, salinity and pressure, Fig. 5.

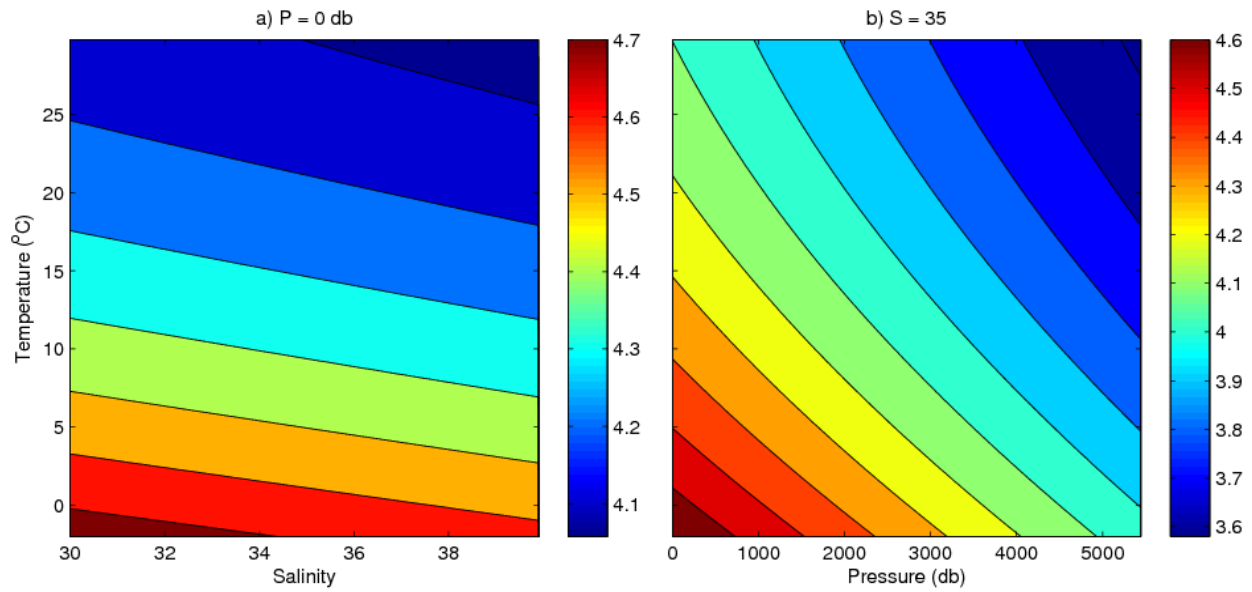


Fig. 5. Compressibility ($10^{-6}/\text{dbar}$) as a function of temperature, salinity and pressure.

Most importantly, cold and fresh water is more compressible than warm and salinity water, and cold water at surface is more compressible than warm water at depth. Let us assume that on the same potential surface, potential temperature is higher at the shallow level than that at the deeper level.

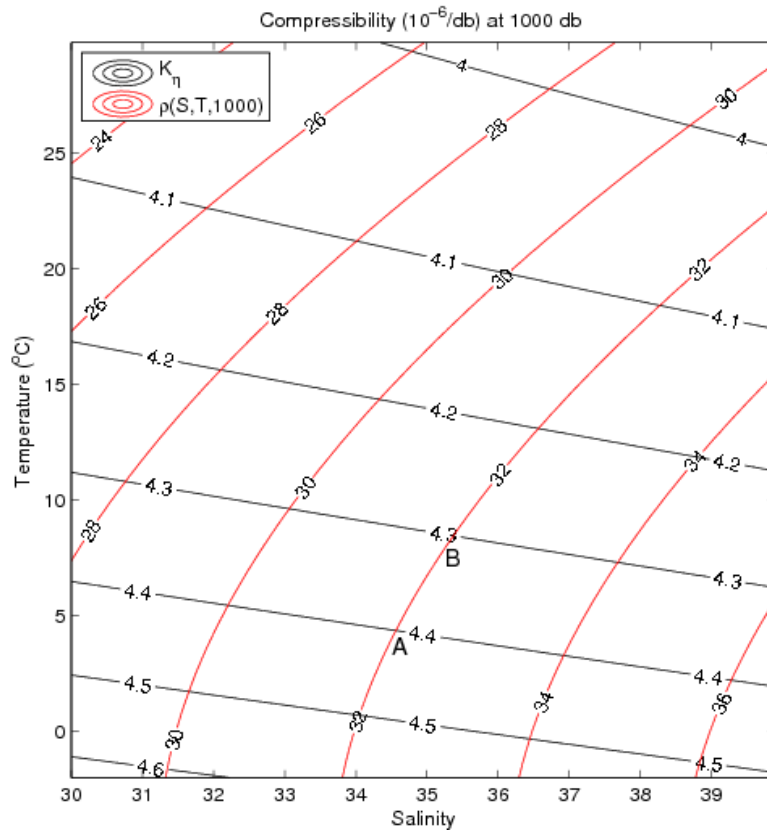


Fig. 6a. Compressibility of sea water at 1000 db.

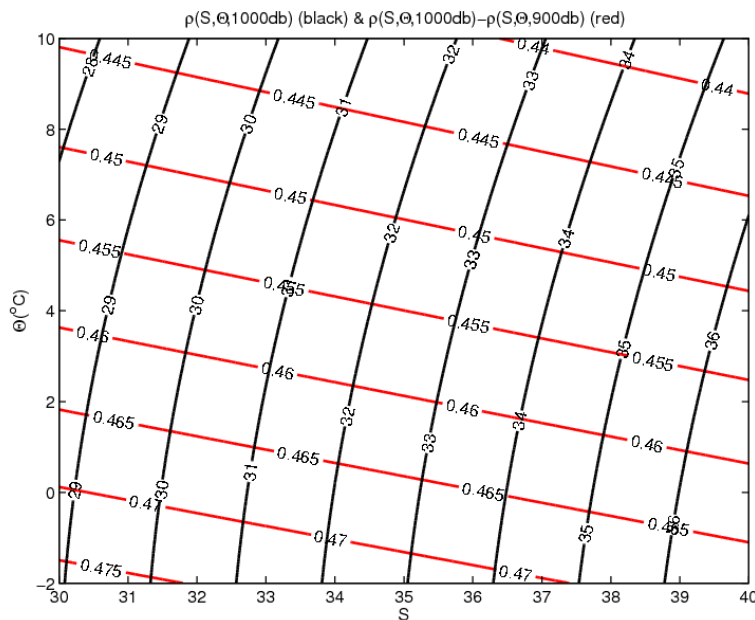


Fig. 6b. In-situ density as a function of potential temperature and salinity at $p=1000\text{db}$ and changes in in-situ density as water parcels move from 900 db to 1000db pressure level.

Let us examine the situation at 1000 db pressure level, Fig. 6a. Take the $\sigma_{1000} = 32.0 \text{ kg / m}^3$ potential density contour, which intersects many compressibility contours. As discussed above, cold and freshwater is more compressible than warm and salty water. Assume that two water parcels, A and B, have the same potential density $\sigma_{1000} = 32.0 \text{ kg / m}^3$, but parcel A is colder and fresher than parcel B. At the 1000db level, their in-situ density is exactly the same. When they move to a shallow pressure level, parcel A should have a density smaller than parcel B because parcel A is more compressible. On the other hand, if they both move to a deeper level, parcel A should have an in-situ density heavier than parcel B.

This point is illustrated further in Fig. 6b, where the black contours indicate in-situ density at 1000 db level as a function of potential temperature and salinity; the red lines indicate the corresponding density decline, if a water parcel is moved from 1000 db level to 900 db level. Since the equation of state of sea water is highly nonlinear, it two water parcels with different potential temperature and salinity have the same in-situ density at 1000 db level, they will not have the same in-situ density at 900 db level. For example, let us take A as the intersection of density contour (black line) 30 and the density change contour (red) 0.47. That mean a water parcel at this point should have an in-situ density of $\sigma = 30 \text{ kg / m}^3$, and at the 900 db level, its density should be reduced to $\sigma = 30 - 0.47 = 29.53 \text{ kg / m}^3$. Take another water parcel B along the $\sigma = 30 \text{ kg / m}^3$ contour, say the intersection with the red contour of $d\sigma = 0.465 \text{ kg / m}^3$. That means at 900 db level, this water parcel should have an in-situ density of $\sigma = 30 - 0.465 = 29.535 \text{ kg / m}^3$. Therefore, these two parcels have different in-situ density at the 900 db level, although they have the same in-situ density at the 1000 db level.

Let us assume that parcel A was originally at p=1000 db level, and B was at p=900 db level. When B travel to the 1000 db level and replaces parcel A, the in-situ density does not change; thus, there is indeed no buoyancy work associated with such a movement, as argued in the classical documents. However, parcel A is now removed from its original position, and the original position of parcel B is now empty. For mass continuity, we must assign a new position for parcel A and fill up the empty lot left by parcel B. An obvious choice is to move parcel A to the old position of parcel B, as suggested in Fig. 1b. However, when parcel A arrives at this new location, its in-situ density is lighter than the original value of parcel B. That means local water column above must be pushed upward to accommodate the slightly larger volume of parcel A. As a result, external mechanical energy is required for switching these two parcels. In summary, the so-called isopycnal mixing or along-neutral surface mixing is involved with buoyancy work, a contrary to the classic concept of neutrality.

Since compressibility is mostly dependent on potential temperature, we can explain the situation clearly from the distribution of depth and potential temperature on a quasi-neutral surface, Figs. 7 and 8.

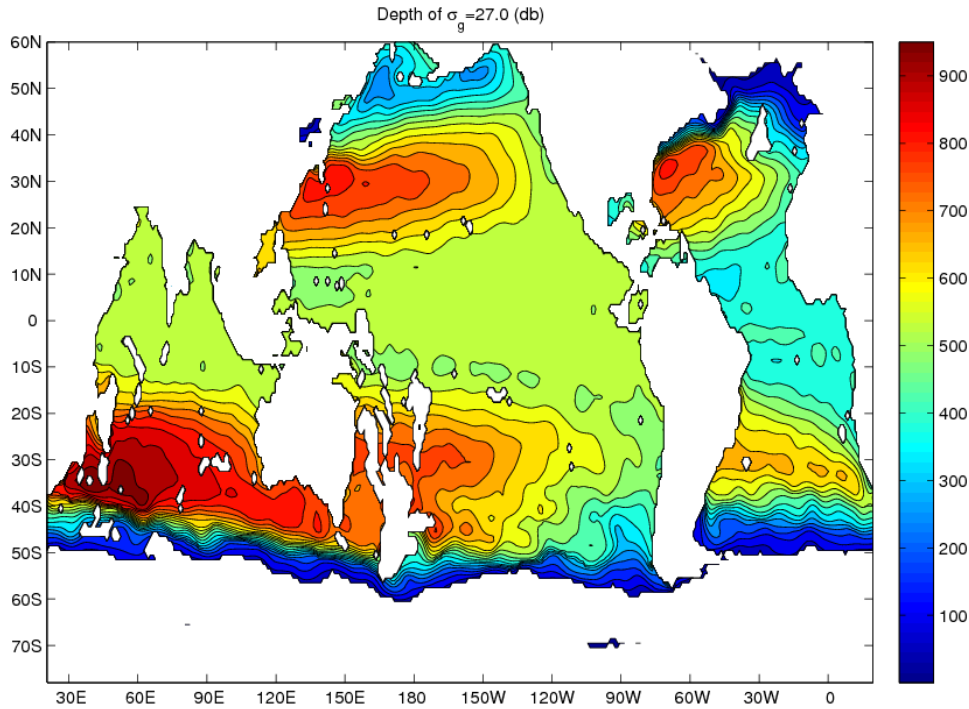


Fig. 7. Depth of the global pressure-corrected density (GPD) surface $\sigma_g = 27.0 \text{ kg} / \text{m}^3$.

It is clear that along the edge of Antarctic Circumpolar Current (ACC), in the southward direction both depth of GPD surface and potential temperature decline. This is situation described in Fig. 3. For the present case, point B (A) in Fig. 6 corresponding to point O (S) in Fig. 3. Assume that a potential density surface passing point B, using pressure at point B as the reference pressure, also passes point A. Thus, in-situ density of parcel A and B at point B should be the same. However, on a shallower pressure level at point A, the in-situ density of parcel B should be heavier than that of parcel A because parcel B is warmer and thus less compressible. As a result, water column at point A should shrink and gravitational potential energy is released.

Similar situation happens for the high latitude parts of both the North Atlantic and North Pacific Ocean, where potential temperature and layer depth decline in the poleward direction; thus, water parcel exchange along quasi-neutral surface and in the meridional direction here is associated with the release of gravitational potential energy.

The situation within the low latitude band is opposite. As shown in Fig. 6, layer depth decline in the equatorward direction; however, potential temperature increases toward the equator, Fig. 8. Such a situation is described in Fig. 4. Now point A (B) in Fig. 6 corresponds to point O (S) in Fig. 4. By definition, parcel B should have the same in-situ density as parcel A, if it is moved to point O. However, if they both are moved to point S along the quasi-neutral surface, parcel A should have an in-situ density smaller than that of parcel B because parcel A is colder and more compressible. Therefore, exchange these two water parcels requires external mechanical energy for supporting.

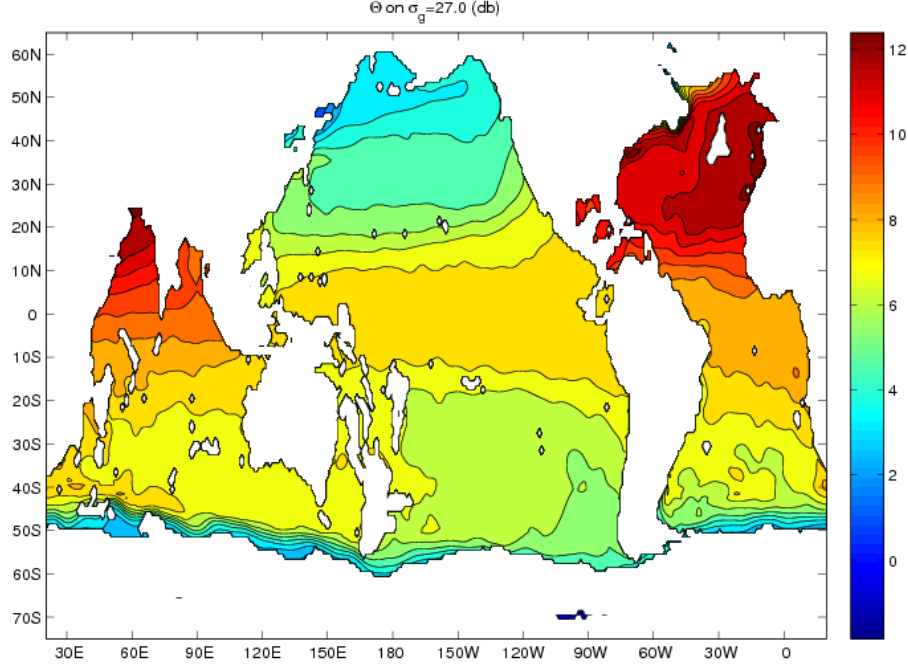


Fig. 8. Distribution of potential temperature on global pressure-corrected density surface $\sigma_g = 27.0 \text{ kg} / \text{m}^3$.

4. GPE change due to parcel exchange along neutral surface

Let us focus on the case discussed in Fig. 4. The pivotal potential surface is set as σ_{1000} , and it intersects at station on pressure level $p_s = 983.578 \text{ db}$. By definition, the in-situ density of parcel O (originally sits at this pressure level) and parcel A at station S (originally sits at pressure level $p_s = 983.578 \text{ db}$) are the same, i.e.,

$$\rho(O) = \rho(A \rightarrow O). \quad (1)$$

However, at pressure level p_s , the density of the parcel O starting from point O is smaller than the in-situ density of the original parcel A by the amount of

$$\delta\rho = \rho(O \rightarrow A) - \rho(A) < 0. \quad (2)$$

Assuming water parcel movements are isentropic, without change of potential temperature and salinity, for small perturbations we have

$$\rho(O \rightarrow A) = \rho(O) + \rho_0 K_\eta(S_o, \Theta_o, p_o) \delta p \quad (3a)$$

$$\rho(A \rightarrow O) = \rho(A) - \rho_0 K_\eta(S_A, \Theta_A, p_A) \delta p \quad (3b)$$

where $\delta p = p_A - p_o = 987.578 - 1000 = -12.422 \text{ db} < 0$. Using condition (1), Eq. (3a) and (3b) lead to

$$\begin{aligned}
\rho(O \rightarrow A) - \rho(A) &= -\rho_0 \left[K_\eta(S_A, \Theta_A, P_A) - K_\eta(S_O, \Theta_O, P_O) \right] \delta p \\
&= -\rho_0 \left[\frac{\partial K_\eta}{\partial \Theta} \delta \Theta + \frac{\partial K_\eta}{\partial S} \delta S + \frac{\partial K_\eta}{\partial p} \delta p \right] \delta p \\
&= -\rho_0 \left[\frac{\partial K_\eta}{\partial \Theta} \frac{\partial \Theta}{\partial p} \Big|_{\bar{n}} + \frac{\partial K_\eta}{\partial S} \frac{\partial S}{\partial p} \Big|_{\bar{n}} + \frac{\partial K_\eta}{\partial p} \Big|_{\bar{n}} \right] \delta p^2
\end{aligned} \tag{4}$$

where ρ_0 is the mean reference density, $\delta \Theta = \Theta_A - \Theta_O$, $\delta S = S_A - S_O$, and \bar{n} is the normal vector shown in Fig. 2.

Assuming that the mass of each water parcel is $\delta m = \rho \Delta h A$, where Δh is the original thickness of the water parcel, and A is the horizontal area of the gird box; then the corresponding change of the layer thickness is $\delta h = -\Delta h \delta \rho / \rho_0 > 0$. Due to the expansion of this water parcel the total water column above pressure level p_s is pushed upward by this distance, and the corresponding increase of gravitational potential energy of the system is estimated as

$$\begin{aligned}
\delta \chi &= p \delta h A = -p \Delta h A \delta \rho / \rho_0 \\
&= p \Delta h A \left[\frac{\partial K_\eta}{\partial \Theta} \frac{\partial \Theta}{\partial p} \Big|_{\bar{n}} + \frac{\partial K_\eta}{\partial S} \frac{\partial S}{\partial p} \Big|_{\bar{n}} + \frac{\partial K_\eta}{\partial p} \Big|_{\bar{n}} \right] \delta p^2 > 0
\end{aligned} \tag{5}$$

Thus,

$$\delta \chi = p \delta h A = p \Delta h A K_{\eta,l} \delta l^2 > 0 \tag{6}$$

where δl is the horizontal gird size, or the distance between centers of these two water parcels,

$$K_{\eta,l} = \left[\frac{\partial K_\eta}{\partial \Theta} \frac{\partial \Theta}{\partial l} \Big|_{\bar{n}} + \frac{\partial K_\eta}{\partial S} \frac{\partial S}{\partial l} \Big|_{\bar{n}} + \frac{\partial K_\eta}{\partial p} \frac{\partial p}{\partial l} \Big|_{\bar{n}} \right] \frac{\partial p}{\partial l} \Big|_{\bar{n}} = \nabla K_\eta \cdot \nabla p > 0 \tag{7}$$

In general, the contributions due to the second and third terms in Eq. (7) are small, so we will be focused on the contribution due to potential temperature distribution. Since cold water is more compressible, i.e., $\partial K_\eta / \partial \Theta < 0$, when the potential temperature increases with decrease of pressure, constraint (7) is satisfied. As an example, in the equatorward edge of the subtropical gyre in the North Pacific, the meridional pressure (depth) gradient is opposite to that of the potential temperature. As a result, in this regime isopycnal mixing requires external source of mechanical energy for supporting. In general, it is clear that in broad regimes of the world oceans, the term in Eq. (7) is non-zero. Wherever $\nabla K_\eta \cdot \nabla p > 0$, external source of mechanical energy is needed for sustaining isopycnal mixing. On the other hand, $\nabla K_\eta \cdot \nabla p < 0$ indicates that gravitational potential energy is reduced due to isopycnal mixing, thus, isopycnal mixing can take place on its own without local external source of energy for supporting.

Assuming this exchange is completed within a time of ΔT , the rate of GPE generation is

$$\Delta \chi / \Delta T = p \Delta h A K_{\eta,l} \delta l^2 / \Delta T \tag{7}$$

The GPE generation rate is

$$\frac{1}{A\delta h} \frac{\delta\chi}{\Delta T} = K_{H,n} \rho K_{\eta,l} \quad (8)$$

where $K_{H,n} = \delta l^2 / \Delta T$ is the horizontal diffusivity in the normal direction as shown in Fig. 2.

Assuming the mechanical energy per unit volume available for horizontal mixing is ε_H , then the horizontal mixing coefficient can be parameterized as

$$K_{H,n} \leq \frac{\alpha_H \varepsilon_H}{\rho K_{\eta,l}} \quad (9)$$

where $\alpha_H \approx o(1)$ is an empirical efficiency of horizontal mixing. This case applied to the equatorial side of the subtropical gyres, as shown in the following figures. However, on the poleward side of the subpolar gyres, potential temperature is lower on the shallower level; thus, the corresponding GPE change due to parcel switching is negative, i.e. mixing along isopycnal can take place freely.

5. Energy sustaining vertical mixing

As a comparison, we examine gravitational potential energy changes due to vertical mixing in the vertical water column, Fig. 10.

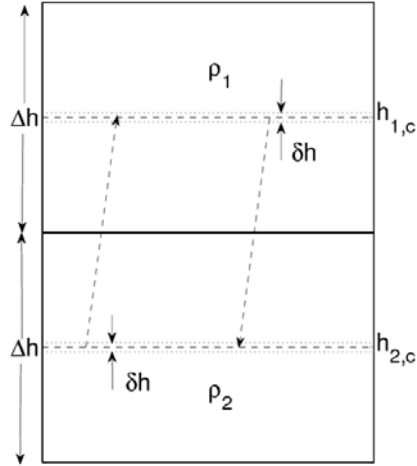


Fig. 9. Sketch of two water parcels involved in vertical mixing.

If we omit the advection terms for simplicity, then the vertical (potential) density balance equation is

$$\frac{\partial \rho}{\partial t} = \frac{\partial F}{\partial z}, \quad F = \kappa \frac{\partial \rho}{\partial z} \quad (10)$$

The dimension of the density flux is the mass flux per unit area.

$$\left[F = \kappa \frac{\partial \rho}{\partial z} \right] = \frac{L^2}{T} \frac{kg}{L^4} = \frac{kg}{L^2 T} \quad (11)$$

Assume that there are two water parcels (with thickness Δh) line up in a vertical water column, the density of them are ρ_1 and ρ_2 , $\rho_2 > \rho_1$. Over a time of ΔT , a fraction of these two parcel, δh of each parcel, is exchanged. Thus, the mass flux associated with this exchange is $\Delta\rho\delta h$, $\Delta\rho = \rho_2 - \rho_1$

$$(12)$$

The corresponding rate of changes in GPE is

$$\Delta\chi = g\Delta\rho\Delta h\delta h / \Delta T \quad (13)$$

Thus, the equivalent vertical diffusivity is

$$\kappa_v = \frac{\delta h\Delta h}{\Delta T} \quad (14)$$

Due to this mass exchange, the rate of GPE increase per unit volume in this two-parcel system is

$$\frac{1}{A\Delta h} \frac{\Delta\chi}{\Delta T} = \kappa_v g \frac{\Delta\rho}{\Delta h} = -\kappa_v g \rho_z \quad (15)$$

Thus, the vertical diffusivity can be parameterized as

$$\kappa_v \leq \frac{\alpha_v \epsilon_v}{-g\rho_z} \quad (16)$$

where $\alpha_v \approx o(1)$ is an empirical efficiency of vertical mixing. Both Eqs. (9) and (16) can be used as the energy upper bound for the diffusivity used in the oceanic general circulation model. The practical application of this scheme can be implemented through the rotating of the mixing tensor, and this is left for further study.

6. How much energy is linked to the isopycnal mixing?

As discussed above, the rate of gravitational potential energy change associated with horizontal mixing is $K_H p K_{\eta,l}$. A typical value for the horizontal diffusivity used in low resolution oceanic general circulation model is on the order of $K_H = 1000 m^2 / s$. The total amount of wind energy input to the surface current is about 0.8-1 TW, and the amount of gravitational potential energy generated by diapycnal mixing sustained by tidal mixing in the open ocean is about $E_{TM} = 0.18$ TW (Huang, 2010). Therefore, we will use $E_{HM} = 0.1TW$ as the criterion to judge whether energy associated with isopycnal mixing is important or negligible, and the critical value is estimated as

$$C = p K_{\eta,l} \Big|_{critical} = \frac{E_{HM}}{V H_H} = \frac{0.1 \times 10^{12}}{1.3 \times 10^{18} \times 10^3} \approx 10^{-10} J / m^5 \quad (17)$$

As example, we calculated the corresponding distribution of the gravitational potential energy associated with the isopycnal mixing, shown in Figs. 10, 11, 12. These maps are based on the σ_g surfaces; however, any other quasi-neutral surface will give very similar results. IN general, the sink of gravitational potential energy is largest in the southern part of the subtropical gyre in the North Pacific Ocean. It is clear that the amount of energy required for sustaining isopycnal mixing in the ocean is small; however, it may not be completely negligible. On the other hand, the amount of energy released through isopycnal mixing may be an important term in the global energetics of the oceans. The Antarctic Circumpolar Current is the site with the highest rate of gravitational potential energy release. However, the exact rate of the global contribution is left for further study.

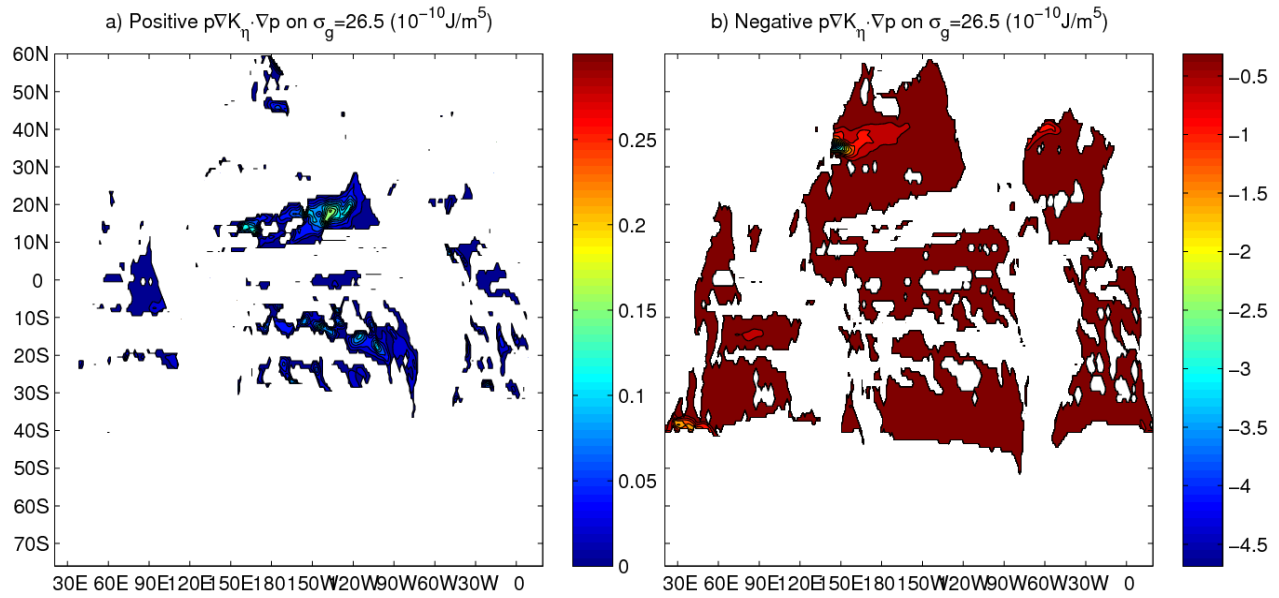


Fig. 10. Gravitational potential energy sink and source associated with isopycnal mixing on $\sigma_g = 26.5$ (kg/m^3) surface.

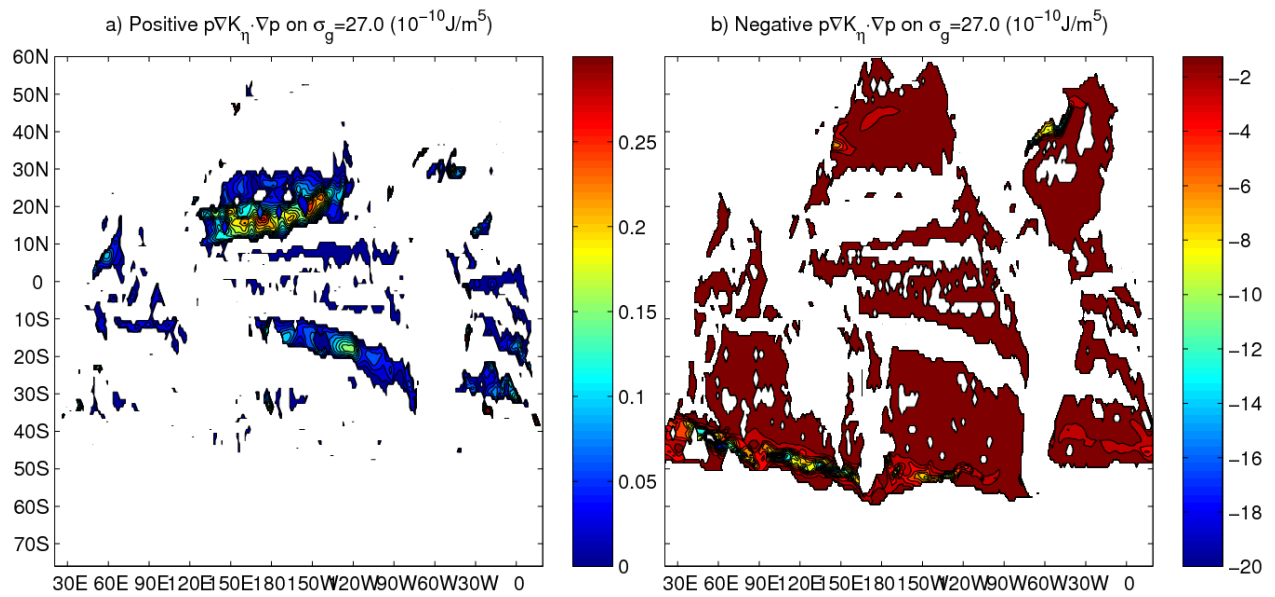


Fig. 10. Gravitational potential energy sink and source associated with isopycnal mixing on $\sigma_g = 27.0$ (kg/m^3) surface.

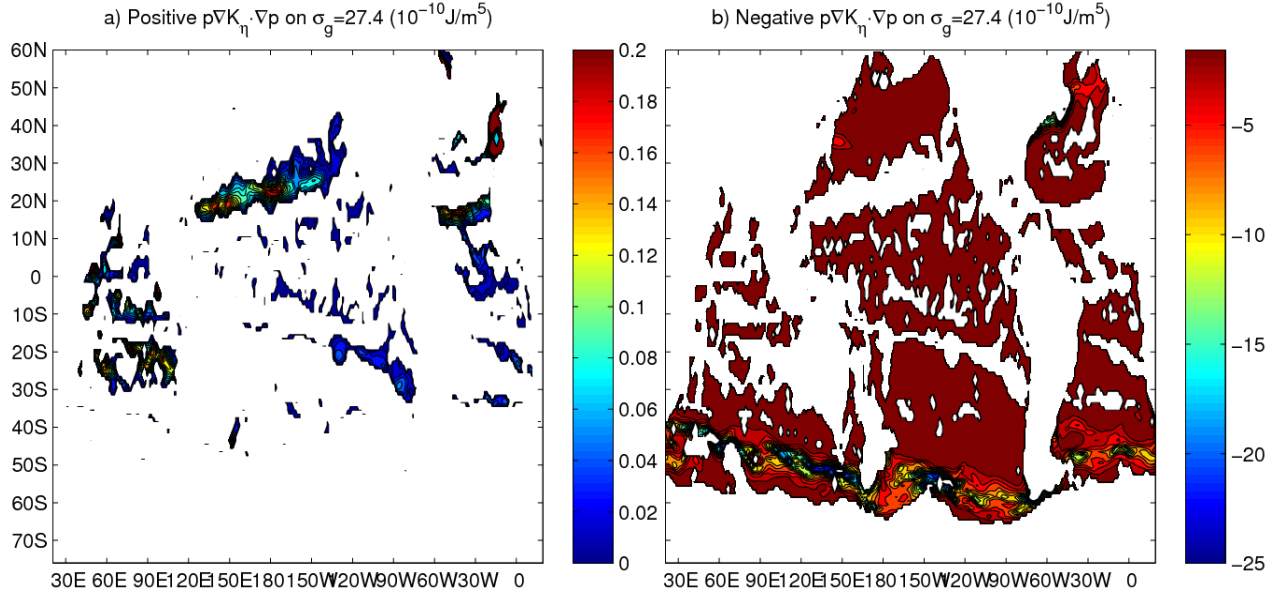


Fig. 12. Gravitational potential energy sink and source associated with isopycnal mixing on $\sigma_g = 27.4$ (kg/m^3) surface.

The last question is how much is the energy associated with isopycnal mixing. Based on the σ_g system, the total amount of gravitational potential energy loss and gain associated with isopycnal mixing is shown in Fig. 13. It is clear that the energy required for isopycnal mixing is relatively large for the density range near $\sigma_g = 27 \text{ kg/m}^3$. However, the total amount of energy is relatively small, on the order of 0.0002TW only.

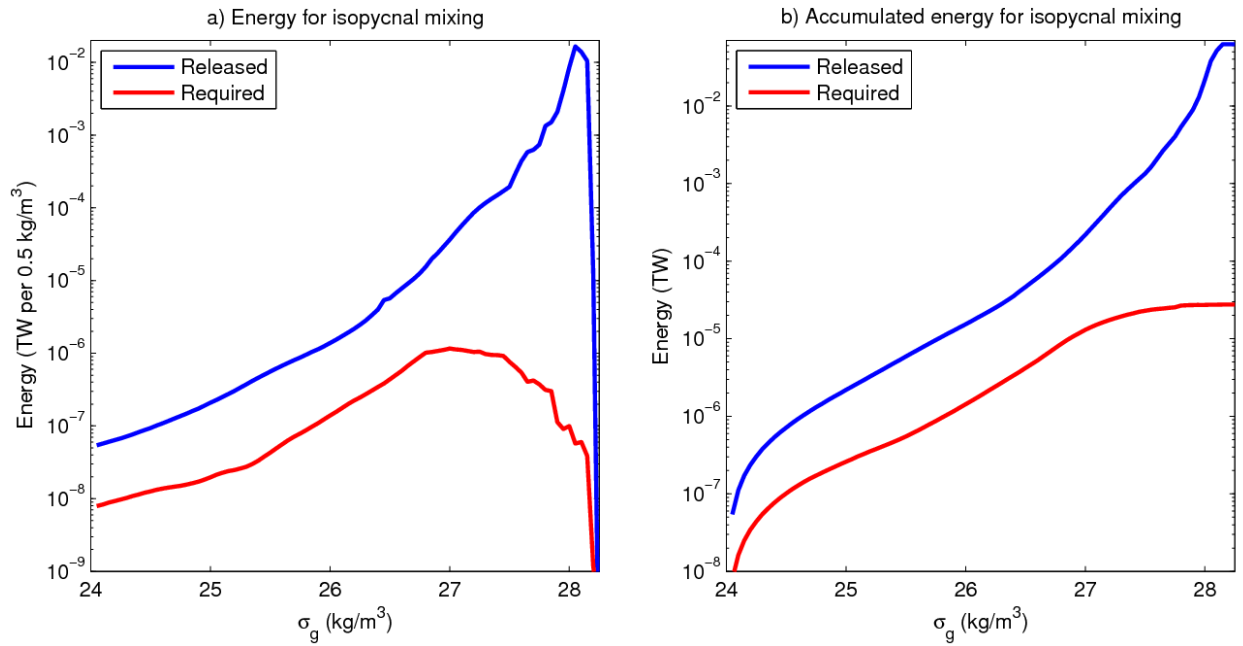


Fig. 13. Energy for isopycnal mixing.

On the other hand, the energy released from isopycnal mixing is quite high for the band of Antarctic Circumpolar Current and the deep ocean, Fig. 13a. The total amount of gravitational potential energy is on the order of 0.06TW. Although this may seem relatively small, it is mostly confined to the southern oceans and the deep ocean, so that this may be comparable with the energy required for diapycnal mixing. The dynamical processes related to the isopycnal mixing and diapycnal mixing are relatively unexplored and this may be one of the most exciting aspects of the oceanic circulation.

7. Conclusion

We explored the energetics of isopycnal mixing through a careful scrutiny of the thermodynamics of sea water. In general, it is clear that on any quasi-neutral surface, both the pressure and the compressibility are not constant; thus, the product of their gradient is non-zero, $\nabla K_\eta \cdot \nabla P \neq 0$. As a result, isopycnal mixing is always associated with change of gravitational potential energy in the system. This change in gravitational potential energy is very strong in the Southern Oceans. It is speculated that this energy release associated with isopycnal mixing in the Southern Ocean may be linked to baroclinic instability and diapycnal mixing in the ocean. A careful exploration along this line may be an important direction to go.

References

- Eden, C. and J. Willebrand, 1999: Neutral density revisited, *Deep-Sea Res. II*, **46**, 33-54.
- Forster, T. D. and E. C. Carmack, 1976. Frontal zone mixing and Antarctic bottom water formation in the southern Weddell Sea, *DeepSea Res.*, **23**, 301-317.
- Huang, R. X., 2010: *Ocean circulation, wind-driven and thermohaline processes*, Cambridge University Press, Cambridge, United Kingdom, 806 pp.
- Jackett, D. and T. J. McDougall, 1997. A neutral density variable for the world's oceans, *J. of Phys. Oceanogr.* **27(2)**, 237-263.
- McDougall, T. J., 1987. Neutral surfaces. *J. Phys. Oceanogr.*, **17**, 1950-1964.